PCCP

Accepted Manuscript

ROYAL SOCIETY OF CHEMISTRY

www.rsc.org/pccp

Journal Name

COMMUNICATION

Intriguing emission properties of triphenylamine-carborane systems

Received 00th January 20xx,
Accepted 00th January 20xx

DOI: 10.1039/x0xx00000x

www.rsc.org/

So-Yoen Kim,[a] Yang-Jin Cho,[a] Guo Fan Jin,[a] Won-Sik Han,[b] Ho-Jin Son,[a] Dae Won Cho[*,a,c] and Sang Ook Kang[*,a,c]

Electron donor-acceptor (D-A) systems with a triphenylamino moiety (D) and *ortho*-carborane (A) show three kinds of intriguing emissions that can be attributed to the local excited state, the intramolecular charge transfer state, and the aggregation induced emission state. The emssion behaviors depend on the substituted positions of carborane.

Electron donor-acceptor (D-A) systems have received much attention in the fields of solar energy conversion and storage,[1–3] molecular electronics,[4] photovoltaics,[5,6] and light-emitting diodes.[7,8] Depending on the application, different types of organic dyes have been developed as the electron donor (D) or acceptor (A). A relatively limited range of molecules has been used as electron acceptor. Among them, perylene bisimides[9,10] and fullerenes[11,12] are representative electron acceptors. o*rtho*-Carborane (*o*-Cb) functions as an excellent electron acceptor[13] when two phenyl units are adjacent through the carbon bonding in the boron-cage.[14–19] Thus, *o*-Cb has been used as the electron acceptor in studies of the photoinduced electron transfer (PET) process.[13] Another issue for D-A dyad formation is the development of an efficient electron donor. Triphenylamine (TPA) has been widely used as the electron donor in optoelectronic materials on account of its good hole-transport mobility.[20–22]

In this study, various D-A dyad and triad systems were prepared using TPA (D) and *o*-Cb (A) as depicted in Scheme 1 (synthetic details in the ESI†). The compounds are: 1-(4-triphenylamine)-2-phenyl-*o*-carborane dyad (**1a**, *p*D-A), 1,2-bis(4-triphenylamine)-*o*-carborane triad (**1b**, *p*D-A-*p*D), 1-(3-triphenylamine)-2-phenyl-*o*-carborane dyad (**2a**, *m*D-A) and 1,2-bis(3-triphenylamine)-*o*-carborane triad (**2b**, *m*D-A-*m*D).

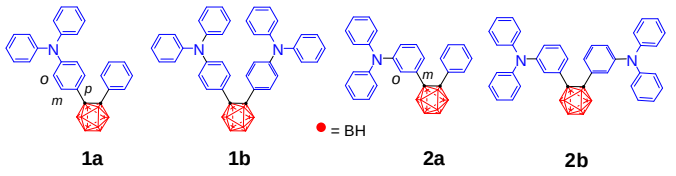

Scheme 1 Molecular structures: blue, donor; red, acceptor.

Solids **1** and **2** are white or light pale-yellow under room light illumination of fluorescent bulbs, as shown in Fig. 1A. However, under UV-illumination with 365 nm radiation, strong red emissions were observed from solids **1** and **2** (Fig. 1b). These can be attributed to aggregation-induced emission (AIE).[23]

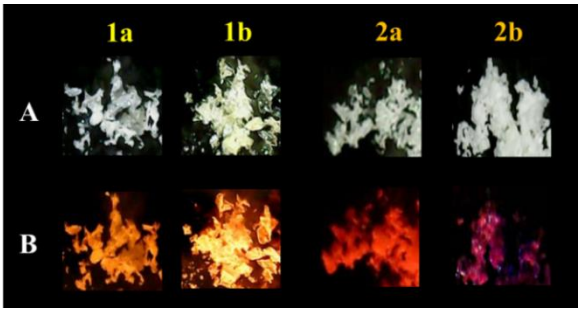

Fig. 1 Photos of compounds **1** and **2** as solid powders under room light (panel A), and fluorescent images under UV illumination (365 nm) (panel B).

Fig. 2 shows the absorbance spectra of **1** and **2** in CH_2Cl_2. As can be seen, **2a** and **2b** having *meta*-substitutions show absorption maxima at 300 nm, which are identical with that of TPA shown in Fig. S1 of the ESI. This means that *o*-Cb does not affect the electronic structure and absorption spectral features of the TPA moiety in the ground state. It is well known that 1,2-diphenylcarborane has an absorption band at around 225 nm.[24] Therefore, the absorption band at 300 nm is attributed to the π–π^* transition of the TPA moiety. Although the absorption maximum wavelength of **2b** is identical to that of **2a**, the absorbance of **2b** is approximately twice that of **2a** because **2b** has two equivalent TPA moieties. This result

[a] Department of Advanced Materials Chemistry, Korea University (Sejong), Sejong, 339-700, South Korea. E-mail: sangok@korea.ac.kr
[b] Department of Chemistry, Seoul Women's University, Seoul 139-774, South Korea.
[c] Center for Photovoltaic Materials, Korea University (Sejong), Sejong, 339-700, South Korea. E-mail: dwcho@korea.ac.kr

† Electronic Supplementary Information (ESI) available: [Synthetic details, absorption and emission spectra of triphenylamine, emission spectra of **1a** in H_2O-CH_3CN, and spectroscopic parameter for **1** and **2**]. See DOI: 10.1039/x0xx00000x

implies that there is a lack of interaction between distant TPA moieties at the *meta*-position.

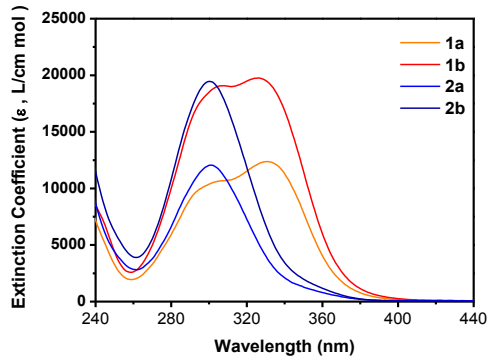

Fig. 2 Absorption spectra for dyads **1** and **2** measured in CH_2Cl_2.

For *para*-substituted compounds, **1a** and **1b**, the absorption spectra shifted to longer wavelengths compared with those of the *meta*-substituted compounds. This bathochromic shift might be attributed to the extension of π-conjugation to the carbon bond of the *o*-Cb moiety. Based on the position of *o*-Cb, the Hammett parameters for a diphenylamine (DPA) substituent are 0.00 (σ_m) and –0.72 (σ_p) for the *meta*- and *para*-positions, respectively.[25] The zero value for σ_m implies a weak electronic interaction between TPA and *o*-Cb moieties at the *meta*-position. Indeed, **2a** and **2b** show similar absorption spectra to that of TPA.

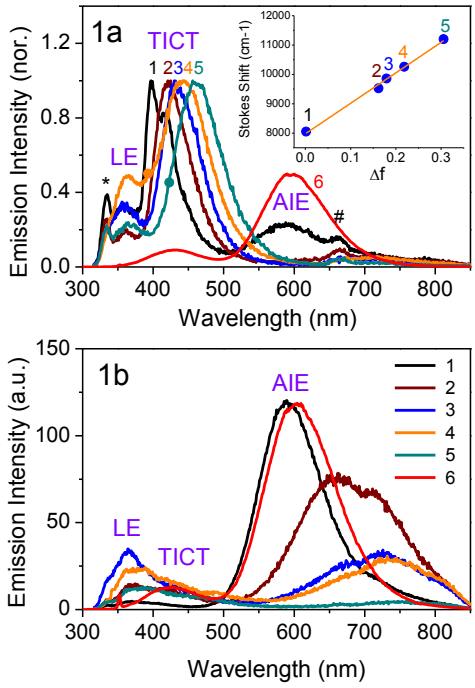

Fig. 3 Emission spectra of **1a** (2.2 μM) and **1b** (4.0 μM) in various solvents: 1, *n*-hexane; 2, ethyl ether; 3, THF; 4, CH_2Cl_2; 5, CH_3CN; and 6, solid. Inset figures indicate the Lippert–Mataga plot. Asterisk and hash marks indicate the Raman signal of the solvent and the second-order peak of the excitation wavelength, respectively. λ_{ex} = 300 nm. Plot 6 for solid samples was measured using a nanosecond pulse of 355 nm (time delay = 20 ns).

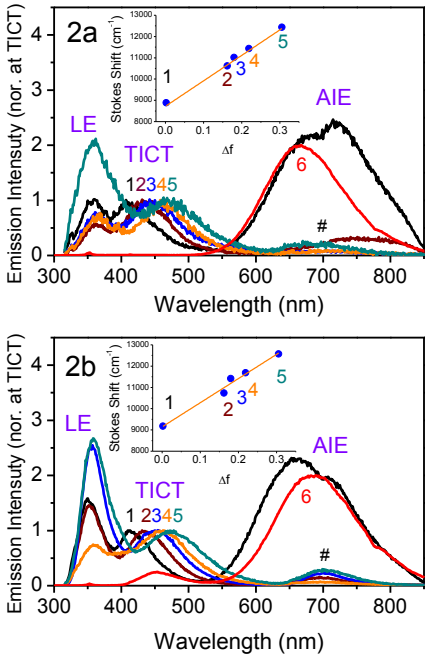

Fig. 4 Emission spectra of **2a** (3.0 μM) and **2b** (1.8 μM) in various solvents: 1, *n*-hexane; 2, ethyl ether; 3, THF; 4, CH_2Cl_2; 5, CH_3CN; and 6, solid. Inset figures indicate the Lippert–Mataga plot. The hash mark indicates the second-order peak of LE emission. λ_{ex} = 300 nm. Plot 6 for solid samples was measured using a nanosecond pulse of 355 nm (time delay = 20 ns).

In contrast to the *meta*-position, the TPA moiety at the *para*-position acts as an electron donor, and the TPA can interact with the *o*-Cb moiety in the ground state, resulting in the broad absorption spectra in Fig. 2. The absorption spectral parameters for **1** and **2** are listed in Tables S1 and S2 in the ESI. The emission spectra of **1a** were recorded in different solvents of increasing polarity from *n*-hexane to CH_3CN. The characteristic dual-emission bands were observed. Among them, the weak emission at 370 nm can be assigned to fluorescence from the local excited (LE) state. The LE emission maxima are not affected by the polarity of the solvent, as shown in Fig. 3. On the other hand, **1a** shows intense emission at around 400 nm in *n*-hexane, which is red-shifted to 460 nm in CH_3CN. The large Stokes shift observed in polar solvents is attributed to the intramolecular charge transfer (ICT) process.

It seems that the salient dual-emission is attributed to some energy barrier between LE and ICT states. This barrier may relate to the geometrical changes in the excited sate. One possible suggestion is a twisted charge transfer (TICT) process. The efficiency of the TICT process is improved when coupled with a conformational change in the molecule. Commonly, in *para*-substituted *p*-(*N,N*-dialkylamino)benzonitrile derivatives, a structural change resulting in a twisted conformation of the dialkylamino group with respect to the benzene ring leads to a TICT state.[26] The occurrence of TICT in the excited state is characterized by a dual fluorescence exhibiting an anomalously large Stokes shift in emission in addition to the normal emission from the LE state. **1** and **2** have the diphenylamino group instead of the dialkylamino group. On the other hand, the lack of evidences of the TICT state for DPA group has been

reported. Moreover, it is reported that the rotational barrier of diphenylamino group is very small, and TPA molecule is too flexible to invalidate the postulated TCIT state.[27] Another possibility is the rotation or flapping motions along the bond between TPA and carborane. Therefore, we suggest that the TICT state be postulated as involving all geometric changes as explained in above.

In contrast to dyad **1a**, the emission spectra of TPA showed no spectral shifts upon changing the solvent polarity, as shown in Fig. S1 of the ESI. It is noteworthy that the TICT emission and its large Stokes shift arise from the presence of the *o*-Cb acceptor. On the other hand, the TICT emission of **1b** was relatively weak. This is because the close proximity of the two TPA moieties in **1b** restricts further rotational movement owing to steric hindrance (Fig. 3).

The LE and ICT emissions were also observed in *meta*-compounds **2a** and **2b** (Fig. 4). Interestingly, the TICT emission is observed even in **2b** because the two TPA moieties at the *meta*-position are far away from each other without any steric hindrance. Based on the Hammett parameter, TPA for the *meta*-position can be classified as a poor electron donor. Therefore, the TICT emissions of **2** are entirely attributed to the electron-withdrawing ability of *o*-Cb.

The TICT emissions of **1a** and **2** gradually shift to longer wavelength with increase in solvent polarity. It is known that the solvent polarity effect can be analysed in terms of the difference in the dipole moments of the ground and excited states, and it has been found that a larger dipole moment change causes a larger Stokes shift. This phenomenon can be analysed using a Lippert-Mataga plot, which is a plot of the Stokes shift of the emission versus the solvent polarity. The difference in the maximum absorption and emission wavelengths, expressed in wavenumbers ($\Delta\bar{\nu}$) is given by the following equation (1):

$$\bar{\nu}_a - \bar{\nu}_f = \left(\frac{2}{hca_0^3}\right)\times\left(\frac{\varepsilon-1}{2\varepsilon+1}-\frac{n-1}{2n+1}\right)\times(\mu_e-\mu_g)^2 = \left(\frac{2}{hca_0^3}\right)\times\Delta f\times(\Delta\mu)^2 \quad (1)$$

where $\mu_e - \mu_g$ ($\Delta\mu$) is the difference between the dipole moments of the excited and ground states, *c* is the speed of light, *h* is Planck's constant, and a_0 is the radius of the Onsager cavity around the fluorophore. The solvent dielectric constant (ε) and refractive index (*n*) are included in the term Δf, known as the orientation polarizability. The Onsager radius (13.45–13.95 Å) was taken as half the average size of the crystal structure for **1** and **2** determined by X-ray crystallography (data not shown). As can be seen in the insets of Figs 3 and 4, the Stokes shift for TICT emissions in various solvents changes linearly with Δf, from which increases in the dipole moments ($\Delta\mu$) for **1a**, **2a**, and **2b** were estimated to be 19.4, 19.0, and 18.6 Debye, respectively. A dipole moment of 4.8 Debye corresponds to a positive charge and an electron held 1 Å apart. Therefore, the observed dipole moment changes indicate that one electron (unit charge) transfers a distance of ~4 Å, which corresponds to the distance between the N atom of the TPA donor and the C atom of the *o*-Cb acceptor.

The broad AIEs of **1** and **2** were observed at around 600–700 nm, especially in *n*-hexane or in solid samples. The AIEs of **1** and **2** show abnormal Stokes shifts of 16,500–19,000 cm^{-1}. The AIE emission of solid **2b** is monitored at a longer wavelength compared with those of the other solid compounds. The large Stokes shift can prevent self-absorption (or self-quenching) in the solid compound. This may produce the bright red emission in the solid state. The AIE maxima of the solid compounds were similar to those measured in *n*-hexane solutions (red lines of 6 in Figs 3 and 4), indicating that the chromophores in the solid state exist in an environment similar to aggregated molecules in a nonpolar solvent such as *n*-hexane. One of the main causes of aggregation for compounds **1** and **2** is their poor solubility in either extremely polar or nonpolar solvents, depending upon whether they themselves are nonpolar or polar, respectively.[28] The AIEs for **1** and **2** were observed easily in *n*-hexane. This means that **1** and **2** have moderately polar properties, making it hard to observe the AIE in a moderately polar solvent such as CH_3CN, but easy in an extremely polar solvent such as water. Control of the water fraction has been used as a method to obtain solid materials that emit a range of colours; indeed, the colour can be tuned by varying the emissive π-electron systems on the *o*-Cb cage scaffold.[29]

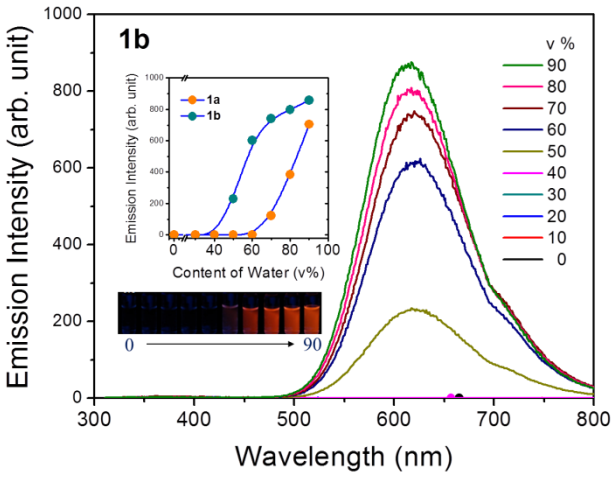

Fig. 5 Emission spectra of **1b** (2 μM) in H_2O–CH_3CN. λ_{ex} = 300 nm. Inset graph: emission intensity of **1a** and **1b** determined at 615 nm in CH_3CN containing water fractions (v/v) in the range 0–90%. Inset photograph: Emission images of **1b** in CH_3CN (0% water) and aqueous mixtures (10−90% water, interval fraction is 10%) under 365 nm UV illumination.

The AIE spectra of **1b** are shown in Fig. 5. Weak emissions for the LE and TICT state are observed in CH_3CN, as mentioned above. When a small amount of water was added (up to ~40%), **1b** did not tend to aggregate. In contrast, when the water fraction was increased above 40%, **1b** started to aggregate and produce red-shifted emission at around 620 nm. The AIE intensity is enhanced with increasing water fraction. The two TPA moieties of **1b** make it a more nonpolar molecule compared with **1a**. Therefore, the AIE of **1b** can be observed at

water fractions above 40% (inset graph of Fig. 5), because the polarity of the solution was increased by adding water. On the other hand, **1a** has moderate polarity compared with **1b**. The AIE is observed in solutions at higher water fractions (>60%) (see inset of Fig. 5 and Fig. S2 in the ESI).

Conclusions

This investigation has uncovered the origins of different types of emissions in D-A systems with a triphenylamino moiety as the donor and *ortho*-carborane as the acceptor. The TICT emissions for **1a**, **2a**, and **2b** were red-shifted with increasing solvent polarity. In contrast, very weak TICT emission was observed from **1b** owing to the close proximity of the two TPA moieties, which restricts further rotational movement owing to steric hindrance. Moreover, AIE emission was observed in all the solid samples and in aqueous CH_3CN solutions. The TICT and AIE emissions were attributed to the introduction of *o*-Cb.

This research was supported by the Basic Science Research Program through the National Research Foundation of Korea (NRF) funded by the Ministry of Education (NRF-2014R1A6A1030732) (S.O. Kang). This work was also supported by the Industrial Core Technology Development Program (10044876) funded by the Ministry of Trade, Industry & Energy (MI, Korea) (S.O. Kang).

Notes and references

1 A. Harriman, M. A. H. Alamiry, J. P. Hagon and D. Hablot, *Angew. Chem., Int. Ed*., 2013, **52**, 6611.
2 M. Urbani, K. Ohkubo, D. M. S. Islam, S. Fukuzumi and F. Langa, *Chem. Eur. J.*, 2012, **18**, 7473.
3 J. E. Bullock, R. Carmieli, S. M. Mickley, J. Vura-Weis and M. R. Wasielewski, *J. Am. Chem. Soc*., 2009, **131**, 11919.
4 D. M. Guldi, *Angew. Chem., Int. Ed.*, 2010, **49**, 7844.
5 G. Bottari, G. de la Torre, D. M. Guldi and T. Torres, *Chem. Rev*., 2010, **110**, 6768.
6 A. Mishra and M. K. R. Fischer, *Angew. Chem., Int. Ed*., 2009, **48**, 2474.
7 J. M. Hancock, A. P. Gifford, Y. Zhu, Y. Lou and S. A. Jenekhe, *Chem. Mater*., 2006, **18**, 4924.
8 G. Hughes and M. R. Bryce, *J. Mater. Chem*., 2005, **15**, 94.
9 W. Jiang, L. Ye, X. Li, C. Xiao, F. Tan, W. Zhao, J. Hou and Z. Wang, *Chem. Commun*., 2014, **50**, 1024.
10 J. Zhang, M. K. R. Fischer, P. Bäuerle and T. Goodson III, *J. Phys. Chem. B*, 2013, **117**, 4204.
11 C. –Z. Li, H. –L. Yip and A. K. –Y. Jen, *J. Mater. Chem*., 2012, **22**, 4161.
12 S. Fukuzumi and T. Kojima, *J. Mater. Chem*., 2008, **18**, 1427.
13 a) K. –R. Wee, W. –S. Han, D. W. Cho, S. Kwon, C. Pac and S. O. Kang, *Angew. Chem., Int. Ed.*, 2012, **51**, 2677; b) G. F. Jin, Y. –J. Cho, K. –R. Wee, S. A. Hong, I. –H. Suh, H. –J. Son, J. –D. Lee, W. –S. Han, D. W. Cho and S. O. Kang, *Dalton Trans*., 2015, **44**, 2780.
14 B. P. Dash, R. Satapathy, B. P. Bode, C. T. Reidl, J. W. Sawicki, A. J. Mason, J. A. Maguire and N. S. Hosmane, *Organometallics*, 2012, **31**, 2931.
15 F. Lerouge, A. Ferrer-Ugalde, C. Viñas, F. Teixidor, R. Sillanpää, A. Abreu, E. Xochitiotzi, N. Farfán, R. Santillan and R. Núñez, *Dalton Trans*., 2011, **40**, 7541.
16 B. P. Dash, R. Satapathy, E. R. Gaillard, K. M. Norton, J. A. Maguire, N. Chug and N. S. Hosmane, *Inorg. Chem*., 2011, **50**, 5485.
17 A. R. Davis, J. J. Peterson and K. R. Carter, *ACS Macro Lett.*, 2012, **1**, 469.
18 K. Kokado, A. Nagai and Y. Chujo, *Macromolecules*, 2010, **43**, 6463.
19 J. J. Peterson, M. Werre, M. Y. C. Simon, E. B. Coughlin and K. R. Carter, *Macromolecules*, 2009, **42**, 8594.
20 Y. Tao, Q. Wang, Y. Shang, C. Yang, L. Ao, J. Qin, D. Ma and Z. Shuai, *Chem. Commun*., 2009, 77.
21 A. Goel, M. Dixit, S. Chaurasia, A. Kumar, R. Raghunandan, P. R. Maulik and R. S. Anand, *Org. Lett*., 2008, **10**, 2553.
22 Z. Ning and H. Tian, *Chem. Commun*., 2009, 5483.
23 R. Hu, N. L. C. Leung and B. Z. Tang, *Chem. Soc. Rev.*, 2014, **43**, 4494.
24 S. Inagi, K. Hosoi, T. Kubo, N. Shida, and T. Fuchigami, *Electrochem*., 2013, 81, 368.
25 C. Hansch, A. Leo and R. W. Taft, *Chem. Rev*., 1991, 97, 165.
26 K. Rotkiewicz, K. H. Grellman and Z. R. Grabowski, *Chem. Phys. Lett*., 1973, **19**, 315.
27 M. Koenig, G. Bottari, G. Brancato, V. Barone, D. M. Guldi and T. Torres, *Chem. Sci*., 2013, **4**, 2502.
28 D. W. Cho and D. W. Cho, *New J. Chem*., 2014, **38**, 2233.
29 M. Tominaga, H. Naito, Y. Morisaki and Y. Chujo, *New J. Chem.*, 2014, **38**, 5686.